Vortex pinning by a columnar defect in planar superconductors with point disorder

Anatoli Polkovnikov, Yariv Kafri, and David R. Nelson
Physics Department, Harvard University, Cambridge, Massachusetts 02138, USA
(Received 21 September 2004; published 14 January 2005)

We study the effect of a single columnar pin on a $(1+1)$-dimensional array of vortex lines in planar type-II superconductors in the presence of point disorder. In large samples, the pinning is most effective right at the temperature of the vortex glass transition. In particular, there is a pronounced maximum in the number of vortices which are prevented from tilting by the columnar defect in a weak transverse magnetic field. Using renormalization group techniques we show that the columnar pin is irrelevant at long length scales both above and below the transition, but due to very different mechanisms. This behavior differs from the disorder-free case, where the pin is relevant in the low-temperature phase. Solutions of the renormalization equations in the different regimes allow a discussion of the crossover between the pure and disordered cases. We also compute density oscillations around the columnar pin and the response of these oscillations to a weak transverse magnetic field.

DOI: 10.1103/PhysRevB.71.014511 PACS number(s): 74.25.Qt, 74.78.−w

I. INTRODUCTION

A key challenge in the physics of vortex line arrays in high-temperature superconductors (HTSC's) is understanding the interplay between vortex interactions and various types of pinning.[1,2] The competition between thermal fluctuations and pinning can lead to different phases such as vortex liquids, Bose and vortex glasses, and a more ordered Bragg glass.[3–7]

Considerable theoretical progress can be made in studying two-dimensional superconductors with an in-plane magnetic field, where the vortex lines form one dimensional arrays. Experimentally this situation can be realized using thin platelet superconducting samples.[8] The statistical mechanics of such systems is equivalent to the physics of interacting bosons in one dimension. The low-energy and long wavelength properties can then be described within a Luttinger-liquid formalism. For example, one can relate the Bose-glass to vortex-liquid phase transition in the presence of disordered columnar defects[3] to the superfluid-insulator transition in a system of interacting bosons with quenched disorder.[9] One finds that for a given disorder strength the system can be tuned across the phase transition by changing the temperature (which is proportional to g, the Luttinger-liquid parameter). The mapping is different with point disorder, which is equivalent to time-dependent point impurities in the boson problem. In this case there is a subtle second order phase transition between a "supersolid" (with algebraic order both in boson and translational order parameter) and glassy phase[5,10–13] with decreasing temperature.

Another important feature of vortex physics in $(1+1)$ dimensions is the remarkable response to a single columnar defect. As argued, originally in the quantum-mechanical context[14] and later for vortex arrays, even a very weak columnar pinning potential can grow to infinity under renormalization group (RG) transformations when $g<1$. It was shown that the relevance of a single columnar pin at low temperatures leads to a strong suppression of a vortex tilt induced by a weak transverse magnetic field. However, at high temperatures (such that $g>1$) the pin is less effective, regardless of its microscopic strength. Remarkably, the onset of the relevance (or irrelevance) of a single columnar pin and point disorder occurs at the *same* temperature $T^\star$, such that $g(T^\star)=1$.

If both point disorder and a columnar pin are present (see Fig. 1) then at low temperatures ($g<1$) one expects a competition between the two: a growing columnar pin strength under renormalization leads to stronger correlated pinning of vortex lines at long length scales. On the other hand, the increasing point disorder tends to destroy the effect of the pin on distant regions. Although it was argued that point disorder would always render a single columnar defect irrelevant at long wavelengths in Ref. 15, the precise nature of this competition and the different pinning properties above and below the vortex glass transition were left unresolved. A detailed study of this competition is a primary goal of the present paper. We show that in the thermodynamic limit the pinning strength is strongest precisely at the transition point $T^\star$ where $g=1$. In particular, the number of pinned vortex lines is a nonmonotonic function of g and strongly peaked at $g=1$. For finite systems the position of the maximum is slightly shifted to lower values of g (see Fig. 4). We emphasize that irrel-

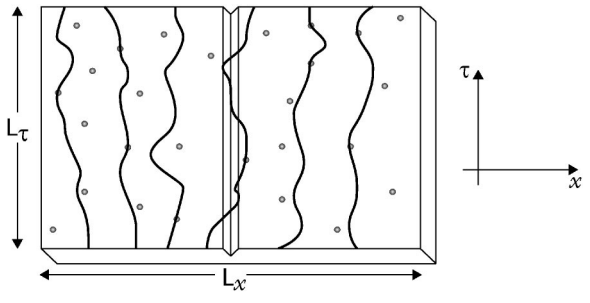

FIG. 1. Schematic view of a planar superconductor with point disorder and a columnar pin, represented by a notch cut into the sample. The wiggly lines correspond to vortices, which alternatively can be thought of as imaginary time world lines of bosons in one spatial dimension.

evance of a single columnar pin does not imply irrelevance of an array of pins. In fact, as it was argued in Refs. 3 and 4, the vortex glass phase formed by point disorder is unstable toward infinitesimal disorder in columnar pins, which results in a Bose glass phase.

The paper is organized as follows. In Sec. II we introduce the model and describe the mapping to a Luttinger liquid. In Sec. III the renormalization equations describing the long wavelength physics are derived. Then in Sec. IV we analyze density oscillations of vortex lines near the columnar pin above and below the vortex glass transition. At the transition point $g=1$, we demonstrate that the problem maps onto free Fermions in a time-dependent disorder potential. This mapping allows computation of density oscillations of vortex lines near the columnar pin which we then compare with the renormalization group predictions. In Sec. V we discuss the response of vortex lines to a weak transverse magnetic field in the presence of a single columnar pin. Finally in Sec. VI we summarize our results and present conclusions. Appendix A estimates the parameter range necessary to see the effects discussed here, while Appendix B describes details of our free fermion calculation.

II. MODEL

A one-dimensional array of vortex lines located at positions $x_j(\tau)$ can be described by the density profile (see Fig. 1)

$$n(x,\tau)=\sum_j \delta[x-x_j(\tau)]. \tag{1}$$

Here x and τ denote transverse and longitudinal coordinates with respect to the vortices. It is convenient to change variables to the phonon displacement field u_j: $x_j(\tau)=a[j+u_j(\tau)]$, where a is the mean distance between the vortex lines. In the absence of a columnar pin, point disorder, and a transverse magnetic field, the free energy of a particular vortex line configuration can then be written as[15]

$$\mathcal{F}_0=\frac{a^2}{2}\int dxd\tau[c_{11}(\partial_x u)^2+c_{44}(\partial_\tau u)^2], \tag{2}$$

where c_{11} and c_{44} are the compressional and the tilt moduli, respectively. After rescaling x and τ

$$x\to x\left(\frac{c_{11}}{c_{44}}\right)^{1/4},\quad \tau\to\tau\left(\frac{c_{44}}{c_{11}}\right)^{1/4}, \tag{3}$$

the free energy takes the isotropic form

$$\mathcal{F}_0=\frac{A}{2}\int dxd\tau[(\partial_x u)^2+(\partial_\tau u)^2], \tag{4}$$

with $A=a^2\sqrt{c_{11}c_{44}}$. The partition function Z describing a vortex array at temperature T is a functional integral over all possible configurations of vortices weighted by a Boltzmann factor proportional to $e^{-\mathcal{F}_0/T}$. In the limit of large sample dimension in a "timelike" direction, Z can also be regarded as the zero temperature partition function of interacting bosons[3,16]

$$Z=\int Du(x,\tau)e^{-S}, \tag{5}$$

with the imaginary time action $S=S_0=\mathcal{F}_0/T$ given by

$$S_0=\frac{\pi}{2g}\int dxd\tau[(\partial_x u)^2+(\partial_\tau u)^2]. \tag{6}$$

For simplicity we here set the Planck's constant $\hbar=1$. Comparison of Eq. (6) with Eq. (4) allows us to identify the Luttinger-liquid parameter g as

$$g=\frac{\pi T}{A}.$$

The rescalings in Eq. (3) are such that the "sound speed" in the Luttinger liquid is equal to 1.

The most relevant contributions to the action from the columnar pin $S_{\rm pin}$ and point disorder S_{PD} read[5,10,13,17]

$$S_{\rm pin}=V_0\int d\tau\cos[2\pi u(0,\tau)], \tag{7}$$

$$S_{PD}=2\int dxd\tau U(x,\tau)\cos[2\pi u(x,\tau)+\beta(x,\tau)], \tag{8}$$

where positive (negative) V and U correspond to repulsive (attractive) potentials. When $V<0$, Eq. (7) represents an attractive columnar pin at the origin. For simplicity we take the phase $\beta(x,\tau)$ to be uniformly distributed between 0 and 2π and $U(x,\tau)$ to have a Gaussian distribution with the correlator

$$\overline{U(x_1,\tau_1)U(x_2,\tau_2)}=\Delta_0\delta(x_1-x_2)\delta(\tau_1-\tau_2), \tag{9}$$

where the overbar represents an average over realizations of the disorder. The total action S entering Eq. (5) is then the sum of the three contributions (6), (7), and (8):

$$S=S_0+S_{\rm pin}+S_{PD}. \tag{10}$$

In the following sections we analyze S and various observables using the renormalization group. Before proceeding with quantitative details we emphasize that although we focus on the behavior of vortex lines in this paper, the action (10) can be relevant for many different problems such as disordered interfaces,[12] charge density waves which order similar to smectic liquid crystals,[18,19] and directed polymer arrays.[20]

III. RENORMALIZATION GROUP FLOW EQUATIONS

Provided one is alert to potential pathologies,[21] an efficient way to analyze disordered problems is to use a replica trick.[22] The noninteracting part of the action (6) then becomes

$$S_0=\frac{\pi}{2g}\sum_{\alpha,\beta}\int\int dxd\tau\left[\frac{\partial u_\alpha}{\partial\tau}\frac{\partial u_\beta}{\partial\tau}+\frac{\partial u_\alpha}{\partial x}\frac{\partial u_\beta}{\partial x}\right]\left[\delta_{\alpha\beta}-\frac{\kappa}{g}\right], \tag{11}$$

where $u_\alpha(x,\tau)$ is the replicated phonon field and κ is an off-diagonal coupling which is zero in the bare model but

generated by the disorder.[11] It is equivalent to (x- and τ-dependent) quenched random "chemical potential" coupled to the first derivatives of the phonon field u.[13,15] The replica indices α and β run from 1 to n and we take the limit $n \to 0$ at the end of the calculation.[11,12] Equation (11) leads to a phonon correlation function in momentum space for $n \to 0$, namely,[11]

$$\langle u_\alpha(k,\omega) u^\star_\beta(k',\omega')\rangle = \frac{4\pi}{k^2+\omega^2}(g\delta_{\alpha\beta}+\kappa)\delta_{k,k'}\delta_{\omega,\omega'}. \quad (12)$$

The other two terms in the action of Eq. (10) corresponding to a pinning potential and point disorder, become

$$S_{\rm pin} = V_0 \sum_\alpha \int d\tau \cos 2\pi u_\alpha(0,\tau) \quad (13)$$

and

$$S_{PD} = -\Delta_0 \sum_{\alpha,\beta} \int\int dx d\tau \cos 2\pi [u_\alpha(x,\tau) - u_\beta(x,\tau)]. \quad (14)$$

To study the statistical physics described by the action (11), (13), and (14) we employ a momentum shell renormalization group scheme,[23] where we continuously eliminate degrees of freedom depending on frequency and momentum within the shell $\Lambda - \delta\Lambda < \sqrt{\omega^2+k^2} < \Lambda$. Here $\Lambda \sim 1/\sqrt{a_0\xi_0}$ is the ultraviolet cutoff, a_0 is of the order of the lattice spacing, and ξ_0 is of the order of superconducting coherence length (single vortex width). The resulting renormalization group equations for the running coupling constants $\Delta(l)$ and $V(l)$ to leading order in Δ and V are

$$\frac{dg}{dl} = 0, \quad (15)$$

$$\frac{d\Delta}{dl} = 2\epsilon\Delta - 2C\Delta^2, \quad (16)$$

$$\frac{d\kappa}{dl} = C^2\Delta^2, \quad (17)$$

$$\frac{dV}{dl} = V(\epsilon - C\Delta) - \kappa V, \quad (18)$$

where $\epsilon = 1-g$, l is the flow parameter [$\Lambda(l) = \Lambda e^{-l}$], and C is a nonuniversal constant which depends on the cutoff Λ: $C \propto 1/\Lambda^2$ (in particular, within the shell method we find $C = 8\pi g^2/\Lambda^2$). These equations are subject to the initial conditions $\kappa(l=0)=0$, $\Delta(l=0)=\Delta_0$, and $V(l=0)=V_0$, with Δ_0 and V_0 being the bare couplings. Note that the Luttinger-liquid parameter g does not change under renormalization.[11]

In the absence of point disorder [$\Delta(l) \equiv 0$ and $\kappa(l) \equiv 0$] our results reduce to those obtained by Kane and Fisher.[14] In this case the columnar pin is relevant for $g<1$ and irrelevant for $g>1$. If $V \equiv 0$ then our equations are equivalent to those first derived by Cardy and Ostlund[11] and later extensively explored for different problems.[5,10,12,13] Equations (15)–(17) imply that point disorder *also* becomes relevant when $g<1$. Contrary to bosons interacting with many impurities[9] (which is the analogue of many *columnar* defects for a flux problem), there is an intermediate fixed point with a finite value $\Delta^\star \equiv \lim_{l\to\infty}\Delta(l) = O(\epsilon)$ which continuously emerges from a pure Gaussian fixed point for $g<1$. This makes the RG approach tractable on both sides of $g=1$. Note also that when $g<1$, $\kappa(l) \to \infty$, suggesting nontrivial correlations in this phase. We comment that there are some claims questioning the applicability of Eqs. (15)–(17) in the glass phase ($g<1$). In Ref. 25 it was argued that a replica symmetric solution becomes unstable for $g<1$, resulting in different correlation functions than predicted by the replica symmetric renormalization group. However, there is still no evidence showing that this instability actually occurs. Moreover, numerical results of Ref. 26 confirm one of the crucial predictions of Eqs. (15)–(17) at $g<1$; namely, the unusual behavior of the density-density correlation function $G(x) \propto \exp(-A\ln^2|x|)$.

In deriving Eqs. (16)–(18), we implicitly assumed that the cutoff is symmetric in the τ and x directions. In general this is not true. The anisotropy in the cutoff will result in different initial renormalizations of κ_τ and κ_x. However, at large length scales the flows for κ_τ and κ_x look the same and the asymmetry disappears.[13]

Equations (15)–(18) contain nonuniversal cutoff dependent terms. Upon rescaling the disorder potential $\Delta \to \tilde{\Delta}/C$ they simplify to

$$\frac{dg}{dl} = 0, \quad (19)$$

$$\frac{d\tilde{\Delta}}{dl} = 2\tilde{\Delta}(\epsilon - \tilde{\Delta}), \quad (20)$$

$$\frac{dV}{dl} = V(\epsilon - \tilde{\Delta}) - \kappa V, \quad (21)$$

$$\frac{d\kappa}{dl} = \tilde{\Delta}^2. \quad (22)$$

These are the renormalization equations which we will exploit throughout the rest of the paper. Note that the cutoff Λ enters Eqs. (19)–(22) only through the initial disorder strength $\tilde{\Delta}_0$.

The quantitative predictions of the renormalization group equations above are valid if $\tilde{\Delta}_0$ is small compared to one. On the other hand if the point disorder is too weak, then its effects will be hard to observe in experiments. In Appendix A we show that for HTSC superconducting films, typical values of point disorder strength lie within interval $\tilde{\Delta}_0 \in [0.01, 0.1]$. This, in turn, implies experimental relevance of the subsequent analysis of the physics resulting from Eqs. (19)–(22) in the different regimes.

High-temperature phase ($g>1$). If ϵ is large and negative ($|\epsilon| \gg \Delta_0$) then both point disorder and pinning strengths decay exponentially to zero as

$$\tilde{\Delta}(l) \sim \tilde{\Delta}_0 e^{-2|\epsilon|l} \to 0, \tag{23}$$

$$V(l) \sim V_0 e^{-|\epsilon|l} \to 0. \tag{24}$$

However, the off-diagonal stiffness κ renormalizes to a finite nonuniversal value

$$\kappa(l) \approx \frac{\tilde{\Delta}_0^2}{4|\epsilon|}(1 - e^{-4|\epsilon|l}) \to \frac{\tilde{\Delta}_0^2}{4|\epsilon|}. \tag{25}$$

As we will see below, the finite value of $\kappa(l=\infty)$ (which arises for any $\epsilon \leqslant 0$) results in corrections to the power law decay of various correlation functions.

Critical phase ($g=1$). When $\epsilon=0$ (i.e., $g=1$), point disorder becomes marginally irrelevant, and one finds

$$\tilde{\Delta}(l) = \frac{\tilde{\Delta}_0}{1 + 2l\tilde{\Delta}_0} \to 0, \tag{26}$$

$$V(l) = \frac{V_0}{(1 + 2l\tilde{\Delta}_0)^{1/4}} e^{-l\tilde{\Delta}_0/2} \to 0, \tag{27}$$

$$\kappa(l) = \frac{\tilde{\Delta}_0 - \tilde{\Delta}(l)}{2} \to \frac{\tilde{\Delta}_0}{2}. \tag{28}$$

Note that even though the point disorder $\tilde{\Delta}$ is marginal at $g=1$, the pinning potential V remains irrelevant [i.e., $V(l) \to 0$] for any nonzero $\tilde{\Delta}_0$.

Low-temperature phase ($g<1$). In the case $\epsilon>0$ we find the following solutions of the flow equations

$$\tilde{\Delta}(l) = \frac{\epsilon \tilde{\Delta}_0}{\tilde{\Delta}_0 + (\epsilon - \tilde{\Delta}_0)e^{-2\epsilon l}} \to \epsilon, \tag{29}$$

$$\kappa(l) = \frac{\epsilon}{2} \ln\left[1 + \frac{\tilde{\Delta}_0}{\epsilon}(e^{2\epsilon l} - 1)\right] + \frac{\tilde{\Delta}_0 - \tilde{\Delta}(l)}{2} \to \epsilon^2 l \to \infty. \tag{30}$$

Note that $\kappa(l)$ grows without bound. The explicit mathematical expression for the renormalized columnar pinning potential is rather complicated. However, one can write the asymptotic form of $V(l)$ at large and small l:

$$V(l) \approx \begin{cases} V_0 \exp(\epsilon - \tilde{\Delta}_0)l, & l \ll l_0, \\ V' \exp\left[\left(\dfrac{\epsilon - \tilde{\Delta}_0}{2} - \dfrac{\epsilon}{2}\ln\dfrac{\epsilon}{\tilde{\Delta}_0}\right)l - \epsilon^2 l^2\right], & l \gg l_0. \end{cases} \tag{31}$$

Therefore as $l \to \infty$, $V(l) \to 0$ *faster* than exponentially in l. Here, l_0 represents a crossover scale

$$l_0 \approx \frac{1}{2|\epsilon|} \ln \frac{|\epsilon - \tilde{\Delta}_0|}{\tilde{\Delta}_0} \tag{32}$$

and

$$V' = V_0 \exp\left[\frac{1}{4}\ln\frac{\epsilon}{\tilde{\Delta}_0} - \frac{1}{4}\mathrm{Li}_2\left(1 - \frac{\epsilon}{\tilde{\Delta}_0}\right)\right], \tag{33}$$

where $\mathrm{Li}_2(x)$ is the polylog function.[24] In the limit $\epsilon \gg \tilde{\Delta}_0$ we can use the asymptotic expansion for $\mathrm{Li}_2(x)$ and get

$$V' \approx cV_0 \exp\left(\frac{1}{4}\ln\frac{\epsilon}{\tilde{\Delta}_0} + \frac{1}{8}\ln^2\frac{\epsilon}{\tilde{\Delta}_0}\right), \tag{34}$$

where c is a number of the order of 1. Note that even though a term of the order of ϵ^2 appears in Eq. (31), its presence is justified. Indeed, according to Eq. (22), at large l we have $\kappa \propto \Delta^{\star 2} l \sim \epsilon^2 l$. It is easy to see that higher order corrections in ϵ to the renormalization group flow equations [in particular to Eq. (20)] will result in terms of the order of $O(\epsilon^3)$ in Eq. (30).

The parameter l_0 defined in Eq. (32) sets a characteristic length scale $\Lambda^{-1}e^{l_0}$, separating long and short length behavior of the pinning potential. As we find below, it also determines the behavior of various observables. Thus, for $\epsilon>0$, at small l the pinning potential first grows under the RG transformations to the value $V_{\max} \approx V(l_0) \approx V_0\sqrt{\epsilon/\tilde{\Delta}_0}$. Then, for larger l, $V(l)$ goes to zero faster than exponentially. We comment that for $g>1$, l_0 sets the characteristic scale beyond which $\Delta(l)$ becomes negligibly small and $\kappa(l)$ stops renormalizing.

Note that the columnar pin is asymptotically irrelevant in the presence of point disorder for all values of g. The mechanisms, which lead to this are different below and above the vortex glass transition. Thus in the high-temperature phase $g \geqslant 1$ thermal fluctuations are responsible for the irrelevance of V at $l \to \infty$. In contrast, in the low-temperature glass phase $g<1$ point disorder is the cause of the flow of V to zero at large l. The distance when the columnar pin starts feeling effects of point disorder and becomes irrelevant grows with decreasing $\tilde{\Delta}_0$. As discussed below, in infinite samples, the effect of the columnar pin is strongest (least irrelevant) precisely at $g=1$.

In the weak disorder limit one can compute various correlation functions using the renormalization group analysis sketched above. In what follows we will discuss several quantities of interest.

IV. DENSITY OSCILLATIONS AND THE FREE FERMION LIMIT

A. Density oscillations near a columnar pin

Since the columnar pinning potential is always irrelevant when point disorder is present, it can be treated perturbatively at sufficiently large length scales. The leading contribution to the "Friedel oscillations" of the density of vortex lines in linear response in V_0 is given by

$$\overline{\langle \delta n(x) \rangle} \approx V_0 \cos 2\pi n_0 x \int_{-\infty}^{\infty} f(x,\tau)\, d\tau, \tag{35}$$

where the angular brackets represent the thermal average and the overbar signifies an average over different configurations of point disorder. The quantity

$$\delta n(x) = n(x) - n_0 \tag{36}$$

is the deviation of the vortex lines density from the mean $n_0 = 1/a$ [see Eq. (1)]. The function $f(x,\tau)$ is defined as

$$f(x,\tau) = \overline{\langle e^{2\pi i[u(x,\tau)-u(0,0)]}\rangle}. \tag{37}$$

We note that $f(x,\tau)$ is proportional to the density correlation function without the columnar pin: $\langle \delta n(x,\tau)\delta n(0,0)\rangle \propto \cos[2\pi n_0(x)] f(x,\tau)$. Explicitly, one finds

$$f(x,\tau) \approx e^{-2\int_0^\infty dl[g+\kappa(l)][1-J_0(re^{-l})]}, \tag{38}$$

where $r = \sqrt{x^2+\tau^2}\Lambda$ is the distance between the two points measured in the units of the original cutoff Λ. The Bessel function $J_0(x)$ appearing in Eq. (38) and in other formulas below is nonuniversal and depends on the actual details of the cutoff procedure. Instead of $J_0(x)$ one can use another cutoff function $\tilde{J}(x)$, e.g., a Gaussian, as long as it satisfies general requirements $\tilde{J}(x\to 0)\to 1$ and $\tilde{J}(x\to\infty)\to 0$. If the disorder is absent in Eq. (38), i.e., $\kappa \equiv 0$, we recover the well-known result for the Luttinger liquid $f(x,\tau)\propto r^{-2g}$. If $g \geqslant 1$ then at long distances f is given more generally by $f(x,\tau)\propto r^{-\eta}$,[12] where

$$\eta = 2[g + \kappa(\infty)]. \tag{39}$$

Thus, when point disorder is irrelevant, the exponent of the correlation decay becomes nonuniversal. For $g<1$ the asymptotic expression for f becomes[11,12] $f(x,\tau)\propto e^{-\epsilon^2 \ln^2 x}$.

Upon using Eqs. (35) and (38) we find that the behavior of $\langle \delta n(x)\rangle$ at large distances for $g \geqslant 1$ is

$$\overline{\langle \delta n(x)\rangle} \propto V_0 \frac{\cos 2\pi n_0 x}{x^{\eta-1}}. \tag{40}$$

This equation is valid only for $x \gtrsim \exp(l_0)$, where l_0 is given by Eq. (32). For smaller x the exponent η changes with x. For $g<1$ the crossover is now from power law decaying correlations of the form (40) with $\eta \approx 2g$ for $1 \ll x \ll \exp(l_0)$ to a faster decay

$$\overline{\langle \delta n(x)\rangle} \propto V_0 e^{-\epsilon^2 \ln(x)^2} \tag{41}$$

in the opposite limit $x \gg \exp(l_0)$.

B. Free fermions

If $g=1$ it is well known that using the Jordan-Wigner transformation bosons can be exactly mapped to spinless free fermions.[27] The transformation also holds in the presence of a columnar pin and point disorder. The columnar pin and the point disorder correspond to static and random time-dependent potentials, respectively. The time-dependent Hamiltonian which describes the fermions then reads

$$\mathcal{H}_f(x,\tau) = -\frac{1}{2m}\frac{d^2}{dx^2} + U(x,\tau) + V_0(x), \tag{42}$$

where $U(x,\tau)$ is a random potential satisfying

$$\overline{U(x_1,\tau_1)U(x_2,\tau_2)} = \Delta_0 \delta(x_1 - x_2)\,\delta(\tau_1 - \tau_2). \tag{43}$$

The mass m (corresponding to the tilt modulus in the original flux line problem) sets the Fermi velocity $v_f = k_f/m$ (where k_f is the Fermi momentum), which represents the sound velocity in the original boson/vortex problem.

If the sample length L_τ in the timelike direction is large, then the partition function of the vortex array is proportional to an appropriate matrix element of the corresponding quantum problem[28]

$$Z = \langle G|T_\tau e^{-\int_0^\infty d\tau \int dx \mathcal{H}_f(x,\tau)}|G\rangle, \tag{44}$$

where T_τ is the usual (imaginary) time-ordering symbol. This expression is the quantum-mechanical expectation value of the evolution operator calculated in its many-fermion ground state $|G\rangle$, for a given realization of point disorder. If the Hamiltonian $\mathcal{H}_f$ is time independent, then Eq. (44) reduces to the zero-temperature quantum partition function. For N noninteracting fermions the ground state can be written as a Slater determinant of the single particle states. However, because the Hamiltonian $\mathcal{H}_f$ is time dependent, the states forming the Slater determinant will not be the eigenstates of $\mathcal{H}_f$. Instead, they will consist of the N largest eigenvalues of the *evolution operator* (see Appendix B for further details). Once $|G'\rangle$ is known one can easily calculate various observables. Here we consider the vortex line density

$$\overline{\langle n(x)\rangle} = \overline{\frac{1}{Z}\langle G|c^\dagger(x)c(x)|G\rangle}, \tag{45}$$

where $c(x)$ is a fermionic annihilation operator. Sufficiently far from the boundaries at $\tau = 0, L_\tau$, the density profile $\overline{n(x)}$ clearly does not depend on τ.

Since we are dealing with noninteracting particles, one can find the eigenstates of the evolution operator numerically even in the presence of point disorder. We describe details of this calculation in Appendix B. Here we just mention that we discretize both space and time and write the evolution operator as a product of transfer matrices. We take a periodic array of $M=201$ sites in the space direction and of size $L=50$ in the timelike direction. The particle filling factor is taken to be approximately 0.1, so that the ground state eigenfunction $|G\rangle$ is the Slater determinant of the 21 highest eigenstates. We took an odd number of sites to have an exact inversion symmetry around the columnar pin in the finite size system and we took the odd number of eigenstates to avoid complications arising from the double degeneracy of the energy spectrum in the absence of point disorder. A columnar defect of strength $V_0 = 0.1$ is placed in the central site, $x_0 = 101$. Point disorder is modeled by a uniformly distributed uncorrelated random potential on each site of the space-time lattice: $U(x,r) \in [-U_0, U_0]$, so that $\Delta_0 = U_0^2/3$. For the effective mass in Eq. (42) we choose $m=5$ corresponding to a hopping amplitude $J=0.1$ in the discretized model (see Appendix B). For each configuration of disorder we numerically find the ground state $|G\rangle$ and the fermion density and finally average over different realizations of point disorder. In this way we obtain "Friedel oscillations" of density for different values of Δ_0. In Fig. 2 we plot a calculated density profile of vortex

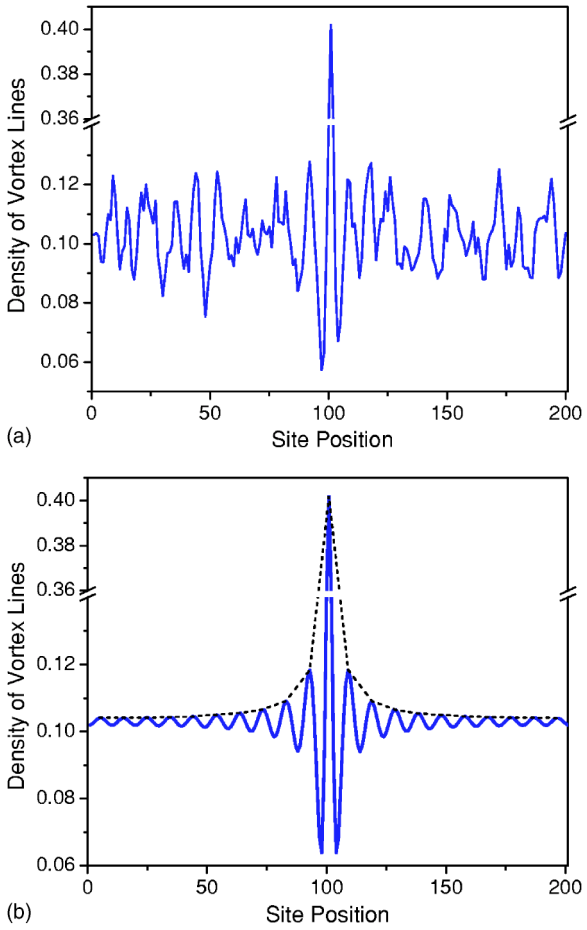

FIG. 2. Density profile of vortex line array near a columnar pin. The top graph (a) shows the result for a single configuration of point disorder. The bottom graph (b) gives the profile after averaging over many disorder realization. The dashed line in the bottom graph shows the envelope of the decay os oscillations, which is used to extract the exponent η [see Eq. (40)].

lines for $U_0=10^{-3/2}$ corresponding to $\Delta_0=3\times10^{-4}$ for a particular realization of point disorder (top graph) and after averaging over about 130 000 disorder realizations (bottom graph). In terms of $\tilde{\Delta}_0$ (23) the chosen strength of point disorder corresponds to

$$\tilde{\Delta}_0 \approx \frac{8\pi\Delta_0}{\Lambda^2} \approx 0.3,$$

where we used the fact that the cutoff is $\Lambda\approx0.1$ for the filling factor 0.1.

Upon fitting the decay of the envelope of oscillations (dashed line in Fig. 2) to a power law [see Eq. (40)] for different strengths of point disorder, we extract the exponent $\eta/2$. The results are plotted in Fig. 3. Within the error bars the dependence of η on Δ_0 is linear as predicted by the renormalization group analysis for $g=1$ [see Eqs. (28) and (39)].

C. Boson phase correlations

Despite the fact that dislocations cannot be present in vortex arrays (as they are equivalent to magnetic monopoles),

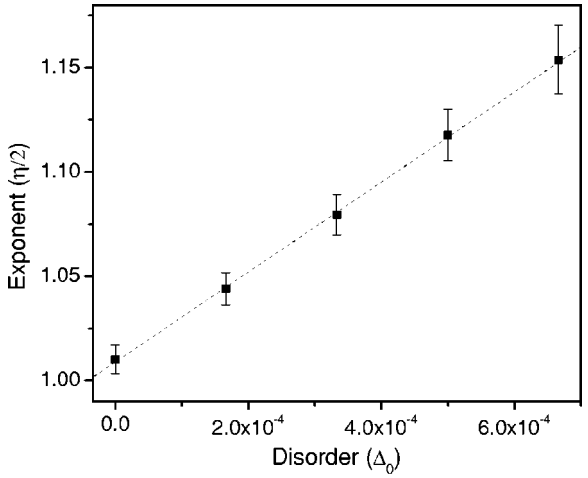

FIG. 3. Extracted exponent $\eta/2$ characterizing decay of density oscillations of vortex lines near a columnar pin [see Eq. (40)] versus the point disorder strength Δ_0. The dashed line represents a linear fit, which agrees with the renormalization group prediction for $g=1$ [see Eqs. (26), (28), and (39)].

they can be relevant for other problems, for example directed polymer arrays in two dimensions. The correlation function, which gives the energy of a dislocation pair[29] (or in the quantum-mechanical language the boson-boson correlation function[17]) can be calculated similarly to the density-density correlation function

$$G(x) = \overline{\langle e^{i[\phi(x,\tau)-\phi(0,\tau)]}\rangle}, \tag{46}$$

where the boson phase angle ϕ is conjugate to du/dx. Upon integrating out ϕ in the standard way, it is easy to show that Eq. (46) can be rewritten as

$$G(x) = \overline{\left\langle \exp\left(-\int_0^x \partial_\tau u(x',0)dx'\right)\right\rangle}. \tag{47}$$

The expression above has to be properly regularized to be cutoff independent. In the absence of a columnar defect, the function $G(x)$ can be straightforwardly calculated as in Eq. (38), yielding

$$G(x) \propto e^{-(1/2g^2)\int_0^\infty dl[g+\kappa(l)][1-J_0(re^{-l})]}. \tag{48}$$

For $g\geqslant1$ at large x this gives

$$G(x) \propto x^{-\eta/4g^2}, \tag{49}$$

where η is defined in Eq. (39). This reduces to the result in the absence of point disorder when $\kappa(l)\equiv0:\zeta(x)\propto x^{-1/2g}$. For $g<1$ as $x\to\infty$ we derive

$$G(x) \propto e^{-\epsilon^2 \ln(x)^2/4g^2}. \tag{50}$$

Since the columnar pin is always irrelevant in the presence of point disorder, it will give only a perturbative correction in V_0 to Eqs. (49) and (50).

Note that the asymptotic behavior of $G(x)$ [Eqs. (49) and (50)] is valid only for an isolated pair of bosons (dislocations in the original problem). It can be shown[11] that under the

renormalization group bosons are relevant on both sides of the transition $g=1$. Thus, if isolated bosons (dislocations) are permitted, they destroy the supersolid-vortex glass transition.

V. RESPONSE TO A TRANSVERSE MAGNETIC FIELD

Another way to determine the effect of a single columnar pin on the flux array is to study the response of the vortices to a weak transverse magnetic field h. In Refs. 17 and 15 it was argued that in the absence of point disorder in the thermodynamic limit an *infinite* number of vortices can be pinned by a single columnar defect in the limit $h \to 0$. While for $g>1$ the fraction of pinned vortex lines goes to zero with the sample size, for $g<1$ almost all lines get pinned. In the presence of point disorder, because the columnar pin is always irrelevant, the situation is quite different. In fact, as we show below, the number of pinned vortices $N_p(g)$ *has a maximum* around $g=1$.

The presence of a transverse magnetic field is manifested through an additional term to the action in Eq. (10) (Refs. 10, 15, and 28)

$$S_m = -\frac{\pi h}{2g}\int dx d\tau \partial_\tau u(x,\tau). \tag{51}$$

It is easy to see that h is formally a relevant variable under renormalization group transformation—in fact its recursion relation is[10] $dh/dl \approx h$. However, when the columnar pin is absent the effect of the transverse magnetic field can be eliminated by a shift of the vortex displacement field $u(x,\tau) \to u(x,\tau) - h\tau$. Clearly, the contribution to the action (after performing the replica trick) coming from point disorder in Eq. (14) is invariant under this transformation. Thus, the only effect of the shift on the action arises from the pinning term (13).

A. Friedel oscillations

The presence of h modifies the decay of the Friedel density oscillations around the pin.[15] It is easy to see that within linear response theory in V_0 the expression (35) transforms to

$$\overline{\langle \delta n(x)\rangle} \approx V_0 \cos(2\pi n_0 x)\int_{-\infty}^{\infty} f(x,\tau)\cos(2\pi h\tau)d\tau. \tag{52}$$

In particular, for $g \geqslant 1$ the density modulation at large distances and weak magnetic fields is readily obtained using Eq. (38):

$$\overline{\langle \delta n(x)\rangle} \propto V_0 \frac{\cos 2\pi n_0 x}{x^{\eta-1}}(hx)^{(\eta-1)/2}K_{(\eta-1)/2}(2\pi hx), \tag{53}$$

where $K_\nu(x)$ is the modified Bessel function of the second kind. One can analyze the asymptotic behavior of Eq. (53) at small and large x. Thus, if $hx \ll 1$ (but $x \gg 1$)

$$\overline{\langle \delta n(x)\rangle} \propto V_0 \frac{\cos 2\pi n_0 x}{x^{\eta-1}}\left[1+\frac{\sqrt{\pi}\Gamma\left(\frac{\eta}{2}\right)(2\pi hx)^{\eta-1}}{\cos\left(\frac{\pi\eta}{2}\right)\Gamma(\eta)\Gamma\left(\frac{\eta-1}{2}\right)}\right]. \tag{54}$$

The second term in the expression above gives a negative correction to the result obtained in the absence of h. In the opposite limit $hx \gg 1$, density fluctuations decay exponentially with x:

$$\overline{\langle \delta n(x)\rangle} \propto V_0 \cos 2\pi n_0 x \frac{h^{\eta/2-1}}{x^{\eta/2}} e^{-2\pi hx}. \tag{55}$$

These findings are consistent with the results of Refs. 15 and 17, where in the pure case when $\eta=2g$. For $g<1$ the situation is more involved. Thus, for $x \ll e^{l_0}$ one can still use Eqs. (54) and (55) with $\eta \sim 2g$. On the other hand if $x \gg e^{l_0}$ the asymptotic behavior of $\langle \delta n(x)\rangle$ is

$$\overline{\langle \delta n(x)\rangle} \propto e^{-\epsilon^2 \ln^2(x)} \tag{56}$$

for a weak magnetic field, $hx \ll 1$. In the opposite limit $hx \gg 1$ we get Eq. (55) with a running exponent η: $\eta(x) \approx \epsilon^2 \ln x$.

B. Number of pinned vortex lines

A much more striking effect of point disorder on the pinning properties of a columnar defect can be observed in the number of vortex lines prevented from tilting by the defect. This "pinning number" is defined as[15,17]

$$N_p(h) = n_0 \frac{\overline{\left\langle \int dx \left(h - \left.\frac{\partial u(x,\tau)}{\partial \tau}\right|_{\tau=0}\right)\right\rangle}}{h}, \tag{57}$$

where as before n_0 is the mean vortex density. This definition can be understood as follows: The numerator is proportional to the difference between the total imaginary currents carried by the vortices in the absence and in the presence of a columnar pin, respectively. Dividing this current difference by the average slope h of the vortex lines in the absence of the pin gives the effective number of vortices which do not participate in the current flow due to the columnar defect. We identify this as the pinning number. It is easy to see that the lowest order correction to the current due to the pinning potential appears in second order perturbation theory. Upon using the simple identity

$$\left.\frac{\partial u(x,\tau)}{\partial \tau}\right|_{\tau=0} = \lim_{\delta\tau\to 0}\frac{e^{2\pi i[u(x,0)-u(x,\delta\tau)]}-1}{2\pi i\,\delta\tau}, \tag{58}$$

we can adopt our previous calculational technique to find

$$N_p \approx \frac{n_0 V_0^2}{4\pi h} \int\int\int d\tau d\tau' dx f(0,\tau-\tau') \left(\frac{\tau R(x,\tau)}{\sqrt{x^2+\tau^2}} - \frac{\tau' R(x,\tau')}{\sqrt{x^2+\tau'^2}} \right) \sin[2\pi h(\tau-\tau')], \quad (59)$$

where

$$R(x,\tau) = \int dl[g+\kappa(l)] e^{-l} J_1(\sqrt{x^2+\tau^2} e^{-l}). \quad (60)$$

Note that if $|\epsilon| \ll 1$ and $\tilde{\Delta}_0 \ll 1$ we can neglect $\kappa(l)$ relative to g in the integral to obtain

$$R(x,\tau) \approx \frac{1 - J_0(\sqrt{x^2+\tau^2})}{\sqrt{x^2+\tau^2}}. \quad (61)$$

After integrating over x we find

$$N_p \approx \frac{g V_0^2 n_0}{4\pi h} \int\int d\tau d\tau' [\mathrm{sgn}(\tau) - \mathrm{sgn}(\tau')] \times f(0,\tau-\tau') \sin 2\pi h(\tau-\tau'). \quad (62)$$

The above integral needs to be handled carefully since it is sensitive to the order of limits. One way to deal with this is to recall that in physical systems the integral over the imaginary time is limited by the sample size $\tau \in [-L_\tau/2, L_\tau/2]$. Then, in Eq. (62) we can make substitutions $\tau \to \tau + \xi/2$, $\tau' \to \tau - \xi/2$ and use the identity

$$\lim_{L_\tau \to \infty} \int_{-L_\tau/2}^{L_\tau/2} d\tau [\mathrm{sgn}(\tau+\xi/2) - \mathrm{sgn}(\tau-\xi/2)] = \xi. \quad (63)$$

In this way our final expression for the number of pinned vortices becomes

$$N_p \approx \frac{g V_0^2 n_0}{4\pi h} \int d\xi \xi f(0,\xi) \sin 2\pi h \xi. \quad (64)$$

Case I, $g \geq 1$. In the high-temperature phase we can use the asymptotic behavior $f(0,\xi) \propto \xi^{-\eta}$ to obtain

$$N_p \propto \frac{V_0^2}{h^{3-\eta}}. \quad (65)$$

In the absence of disorder, $\eta = 2g$ and the expression above agrees with the one obtained in Ref. 15 in the limit $V_0 \ll h$. If the sample size in either the timelike direction L_τ or in the spacelike direction L_x is finite, then at small magnetic fields (64) saturates at

$$N_p \propto V_0^2 L^{3-\eta}, \quad (66)$$

where $L = \min\{L_x, L_\tau\}$. To see this we observe that if L_τ is finite, then the integral over ξ in Eq. (65) is taken within a finite interval $|\xi| \leq L_\tau$. If L_x is bounded then it is easy to show that the correlation function $f(0,\xi)$ decays exponentially $f(0,\xi) \propto e^{-\xi/L_x}$ for $\xi > L_x$ and the integral in Eq. (65) is again cutoff at $\xi \approx L_x$. Note that since with point disorder $\eta > 2$, the fraction of pinned vortices always vanishes in the thermodynamic limit ($L \to \infty$).

Case II, $g < 1$. In the low-temperature vortex glass phase, because of the faster decay of correlations with distance

$$f(0,\xi) \propto e^{-\epsilon^2 \ln^2 \xi}, \quad (67)$$

the number of pinned vortices does not diverge as $h \to 0$. Instead it saturates at

$$N_p \propto \left(\frac{\epsilon}{\tilde{\Delta}_0} \right)^{1/2\epsilon} + \exp\left(\frac{1}{4\epsilon^2} \right). \quad (68)$$

The first term here comes from relatively short distances $\xi \lesssim \exp(l_0)$ and the second one originates from $\xi \gtrsim \exp(l_0)$, where l_0 is defined in Eq. (32). Although $N_p(h)$ remains finite as $h \to 0$ for $g < 1$, note that it becomes very large for $\tilde{\Delta}_0 \ll \epsilon$ and diverges exponentially at $\epsilon \to 0$ at fixed $\tilde{\Delta}_0$.

An important consequence of saturation of N_p at zero tilt with the system size L for $g < 1$ is that as $L \to \infty$, the pinning number will have a maximum as a function of the Luttinger-liquid parameter at $g \approx 1$. If L is not too large (or tilt is finite) then at a given disorder strength the maximum of $N_p(h=0)$ will occur at some $g^* < 1$. Indeed, if g approaches 1 from below, then $N_p(h=0)$ diverges exponentially [see Eq. (68)]. In turn, this implies that if L is finite then the system will be insensitive to the saturating effect of point disorder if g is very close to 1 and the pinning will be quite effective for $g \lesssim 1$ as in the case without point disorder.[17] These simple considerations agree with numerical evaluation of N_p according to Eq. (64), which are plotted in Fig. 4. The position of the maximum (g^*) versus the system size is also shown in this figure. It clearly approaches $g^* = 1$ as L increases. In practice the parameter g can be changed varying vortex line density or temperature.[15,17] Therefore measuring the dependence of the pinning number N_p on g should be experimentally feasible.

VI. CONCLUSIONS

In this paper we studied the effect of point disorder on one dimensional arrays of vortex lines in the presence of a single columnar pin. We obtained the renormalization group flow equations for the pinning strength in the presence of point disorder and found that the columnar pin is irrelevant at the largest length scales (by different mechanisms) both for $g > 1$ and $g < 1$, which is in contrast to the pure system where it is relevant at $g < 1$. Because the onset of relevance of point disorder also occurs at $g = 1$ we were able to quantitatively solve the RG equations for g close to 1. In particular we found that if disorder strength is weak, then at $g < 1$ the renormalized pinning potential V first grows with the increasing length scale to $V_{\max} \approx V_0 \sqrt{(1-g)/\tilde{\Delta}_0}$ and then goes to zero faster than exponentially.

Using renormalization group analysis we calculated "Friedel oscillations" of the vortex line density near the columnar pin. In particular we showed that at $g \geq 1$ density fluctuations decay as a power law $\delta n(x) \propto 1/x^{\eta-1}$, where the exponent η is shifted upwards from $\eta = 2g$ due to point disorder. If $\tilde{\Delta}_0 \ll g - 1$, then the exponent η becomes x independent only at extremely (exponentially) large x. At intermediate x one would observe a power law decay of $\delta n(x)$ with an effective

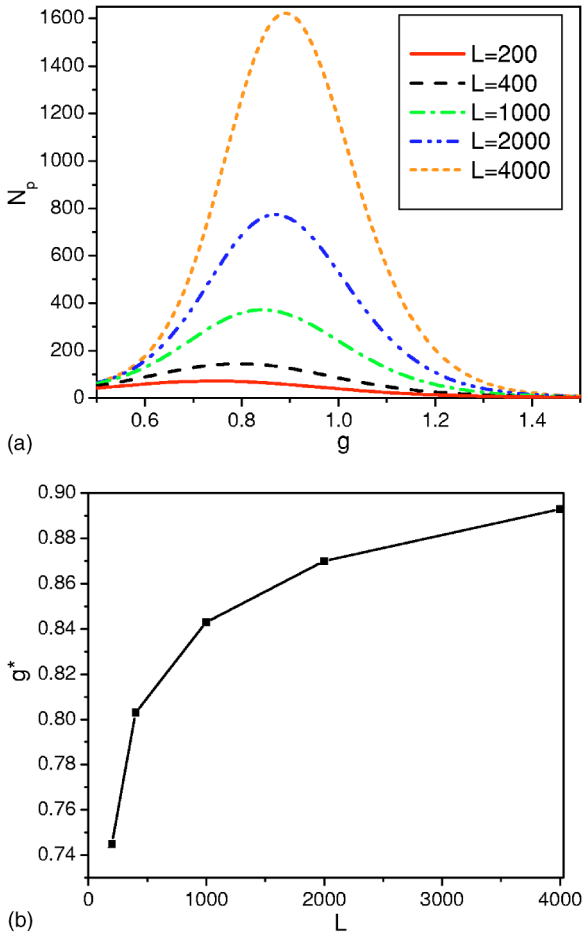

FIG. 4. (Color online) (a) Number of pinned vortices versus the Luttinger-liquid parameter g at a fixed point disorder strength ($\tilde{\Delta}_0=0.2$) for different sample sizes L and (b) the position of the maximum (g^*) as a function of L. The value of g^* approaches 1 with increasing L.

exponent smoothly varying with x. In the case $g=1$ (which corresponds to dilute vortices with a hard core repulsion) we mapped the problem to that of free fermions, which we exactly solved by direct diagonalization. We found that the decay of $\delta n(x)$ in this case agrees with the predictions of our renormalization group analysis. For $g<1$ we showed that the density oscillations at large distances decay faster than a power law $\delta n(x) \propto 1/x^{(1-g)^2 \ln x}$.

We found that the strongest manifestation of point disorder on properties of a single columnar pin is the nonmonotonic dependence of the number of vortex lines prevented by the pin from tilting (N_p) on g in a weak transverse magnetic field. In particular, for $g \geqslant 1$, this number diverges at $h \to 0$ as a power law $N_p \propto h^{\eta-3}$, provided $\eta<3$. In finite systems this divergence is cut off by the system size and N_p saturates $N_p(h=0) \propto L^{\eta-3}$, where L is the smallest of L_x and L_r. The only difference with the pure case is that η gets renormalized by point disorder $\eta>2g$. On the other hand if $g<1$ then arbitrarily weak point disorder leads to saturation of N_p at $h \to 0$. As a result in large samples $L \to \infty$, $N_p(g)$ has a maximum at $g^*=1$, while if L is finite then the maximum occurs at some $g^* \lesssim 1$.

ACKNOWLEDGMENTS

We would like to acknowledge helpful discussions with I. Affleck and W. Hofstetter. Dr. Hofstetter particularly emphasized the mapping to free fermions and shared his ideas on numerical evaluation of the partition function in the presence of point disorder. This work was supported by NSF under Grants Nos. DMR-0233773, DMR-0231631, DMR-0229243 and through the Harvard MRSCC via NSF Grant No. DMR-0213805.

APPENDIX A: ESTIMATES FOR HIGH TEMPERATURE SUPERCONDUCTORS

In this appendix we estimate effects of point disorder discussed above in realistic high-temperature superconductors. The point disorder correlator Δ introduced in Eq. (9) can be estimated as[1,15]

$$\Delta \approx \left(\frac{\Phi_0}{4\pi\lambda}\right)^4 \frac{\xi^3}{T^2 w a^2}\left(\frac{j_c}{j_0}\right)^{3/2}, \tag{A1}$$

where $\Phi_0 \approx 2.07 \times 10^{-7}$ G cm^2 is the flux quantum, λ is the magnetic penetration length, ξ is the superconducting coherence length, w is the sample thickness, and $a=1/n_0$ is the one-dimensional density of vortex lines. Also j_c is the critical current in the presence of point disorder and j_0 is the pair-breaking current ($j_c \approx j_0 \xi^2 n_{\rm imp}^{2/3}$, where $n_{\rm imp}$ is the density of point defects). The factor of $1/w$ in Eq. (A1) appears after averaging over the sample thickness. We are interested at the parameter regime where $g \approx 1$. Then using $\tilde{\Delta} \approx \Delta/\Lambda^2$ (see Sec. III) we get

$$\tilde{\Delta} \approx \left(\frac{\Phi_0}{4\pi\lambda}\right)^4 \frac{\xi^4}{T^2 w a}\left(\frac{j_c}{j_0}\right)^{3/2}. \tag{A2}$$

Let us take the following estimates valid for typical HTSC's: $\lambda=150$ nm, $T=50$ K, $\xi=2$ nm, and $j_c/j_0=0.01$. Following Ref. 8 we also assume that $w \approx \lambda$. Then Eq. (A2) becomes

$$\tilde{\Delta} \approx 10\xi/a. \tag{A3}$$

Quantitative predictions made throughout this paper require that point disorder is relatively weak: $\tilde{\Delta} \ll 1$. Although we expect that arbitrarily large disorder strength renormalizes to zero for $g>1$ and to small values $\tilde{\Delta}^\star \approx 1-g$ for $g \lesssim 1$ [see Eq. (29)], it might be necessary to go to large length scales in order to see this effect. From Eq. (A3) we see that the condition $\tilde{\Delta} \ll 1$ is easily satisfied for magnetic fields below H_{c2} (we recall that in superconducting films with vortices the in-plane magnetic field H is related to the interline spacing a and the film width w through $H \approx \Phi_0/aw$). On the other hand, to be observable, $\tilde{\Delta}_0$ should at least be comparable to $|1-g|$ [see, for example, Eq. (20)]. If the system is tuned within 10% of the vortex glass transition, i.e., $|1-g|=0.1$, then effects of point disorder become relevant for $a \lesssim 100\xi \approx 200$ nm. Such a separation between vortex lines is comparable with the magnetic penetration length λ and thus should be readily accessible at magnetic fields slightly above H_{c1}.

The other quantity crucial to our analysis is the Luttinger parameter g. Interesting and nontrivial effects due to delicate competition between thermal fluctuations and point disorder occur near the vortex glass transition corresponding to $g=1$ (see, for example, Fig. 4). In Ref. 15 it was argued that g may have a nonmonotonic dependence on the vortex line density $n_0=1/a$. In particular, at $a \ll \lambda$ the Luttinger-liquid parameter is very small $g \ll 1$ and in the opposite limit $a \gg \lambda$ we have $g \to 1$. It was also argued in Ref. 15 that at least for some parameter values, increasing the vortex line density causes g to first increase and then decrease to zero. So one might expect that g crosses unity at some intermediate value of a of the order of λ, i.e., around a few hundred nanometers in typical HTSC's. As we showed above, this is precisely what we need to achieve point disorder strength of the order of a few percent. Any necessary fine-tuning of g and $\tilde{\Delta}$ can be achieved slightly varying temperature and the in-plane magnetic field, which determines a.

APPENDIX B: DENSITY OSCILLATIONS OF FREE FERMIONS IN THE PRESENCE OF POINT DISORDER

The partition function of free fermions in a potential with point disorder (assuming for simplicity periodic boundary conditions in the timelike direction) is given by

$$Z = \mathrm{Tr}\langle \Psi | T_\tau e^{-\int_0^{L_\tau} d\tau \int dx \mathcal{H}_f(x,\tau)} | \Psi \rangle, \tag{B1}$$

where Tr denotes the trace over all possible Slatter determinants $|\Psi\rangle$ and $\mathcal{H}_f$ is the Hamiltonian (42) of the noninteracting fermions. A slightly different matrix element is required for vortices with free boundary conditions and finite L_τ. However, in the limit $L_\tau \to \infty$, this detail is irrelevant.[28]

If the Hamiltonian were time independent, then in the zero temperature limit (where in the quantum language temperature is equivalent to $1/L_\tau$) the only contribution to the N-particle partition function comes from the Slatter determinant of N eigenstates of $\mathcal{H}_f$ with lowest eigenenergies (ε_j). Alternatively these are the states, which form the N highest eigenstates of the evolution operator

$$\mathcal{T} = T_\tau e^{-\int_0^{L_\tau} d\tau \int dx \mathcal{H}_f(x,\tau)}. \tag{B2}$$

Note that, in a time-independent problem, nondegenerate eigenvalues λ_j of $\mathcal{T}$ become exponentially separated from each other with increasing L_τ:

$$\frac{\lambda_j}{\lambda_{j+1}} \propto e^{L_\tau(\varepsilon_{j+1}-\varepsilon_j)}. \tag{B3}$$

Therefore, only the largest eigenvalues of the evolution operator need to be considered. We are interested here, however, in the case where the Hamiltonian explicitly depends on time due to point disorder. In this case one can not use eigenstates of $\mathcal{H}_f$, because they also depend on time. However, it is still possible to define the spectrum of the evolution operator for a given L_τ. It seems reasonable to assume that even in the presence of point disorder the separation between the eigenvalues of $\mathcal{T}$ grows exponentially with L_τ.[30] This statement can be checked numerically (see Fig. 5).

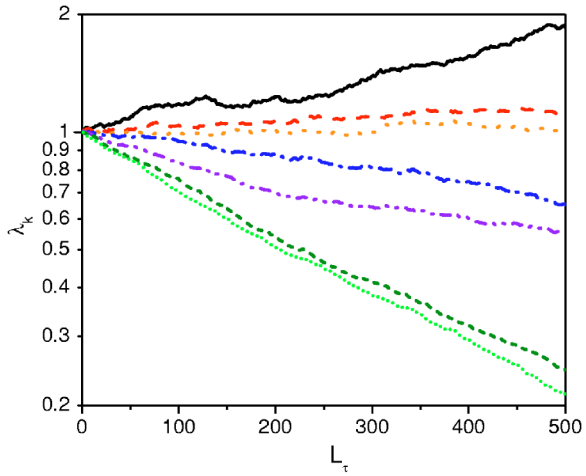

FIG. 5. (Color online) Seven largest eigenvalues of the evolution operator $\mathcal{T}$ as a function of the sample size L_τ. The parameters used in this figure are $L_x=101$, $\Delta_0 \approx 0.008$, $V_0=0.02$, $J=0.1$ [see Eq. (B5)]. For a pure system ($\Delta_0=0$), the largest eigenvalue corresponding to a bound state is followed by three degenerate pairs of smaller ones. Point disorder slightly lifts degeneracy between the states, but clearly does not affect exponential growth of the separation between the pairs of eigenvalues with L_τ.

Therefore, in the limit $L_\tau \to \infty$ the partition function (44) is dominated the "ground state" $|\Psi\rangle = |G\rangle$ of the evolution operator, i.e., by the Slatter determinant of the N highest eigenstates $g_i(x)$ of $\mathcal{T}$:

$$|G\rangle = \det g_i(x_j). \tag{B4}$$

Here $i,j=1,\ldots,N$ enumerate different single particle levels and coordinates. Figure 5 corresponds to relatively strong point disorder and it is necessary to have large sample sizes to assure the ground-state dominance. For weaker disorder it will suffice to have smaller L_τ to find the exponential separation of λ_j.

In order to obtain $|G\rangle$ numerically we discretize the system both in space and time directions. In particular, instead of the Hamiltonian given by Eq. (42) we use

$$\mathcal{H}_f(\tau) = \sum_{j=0}^{M-1} [-J(c_{j+1}^\dagger c_j + c_j^\dagger c_{j+1}) + U_j(\tau) c_j^\dagger c_j] + V_0 c_0^\dagger c_0. \tag{B5}$$

Here $c_j^\dagger$ and c_j are fermion particle creation and annihilation operators, respectively, and M is the number of the sites in the spacelike direction.

We use periodic boundary conditions so that $c_{j+M} \equiv c_j$. The random potential $U_j(\tau_k)$ is taken to be uniformly distributed on each space time point in the interval $[-\sigma,\sigma]$:

$$\overline{U_j(\tau_k) U_i(\tau_p)} = \Delta_0 \delta_{ji} \delta_{kp}, \tag{B6}$$

where $\Delta = \sigma^2/3$. We write the evolution operator as the product

$$\mathcal{T} = \prod_k e^{-\mathcal{H}_f(\tau_k)\delta\tau}. \tag{B7}$$

In order to reproduce the continuum limit (B2), we have to take the time step $\delta\tau$ small enough to ensure that the effects due to $[\mathcal{H}_f(\tau), \mathcal{H}_f(\tau+\delta\tau)] \neq 0$ can be neglected. However, we do not expect any qualitative changes in the results even if this condition is violated. Of course, the time step $\delta\tau$ can ultimately be taken to be 1 by an appropriate scaling of the couplings J, U, and V. In a single particle space both the Hamiltonian $\mathcal{H}_f$ and the evolution operator $\mathcal{T}$ are $M \times M$ matrices. For a given realization of disorder, it is straightforward to diagonalize $\mathcal{T}$ and find its eigenvectors $g_i(x)$ using standard numerical methods. Then the density profile is given by

$$\langle \delta n_d(x_j) \rangle = \sum_{i=1}^{N} |g_i(x_j)|^2. \tag{B8}$$

The index d emphasizes that this is the result for a given realization of point disorder. After averaging $n_d(x_j)$ over disorder realizations we obtain $\langle n(x) \rangle$, which is used in Fig. 3.

[1] G. Blatter, M. V. Feigel'man, V. B. Geshkenbein, A. I. Larkin, and V. M. Vinokur, Rev. Mod. Phys. **66**, 1125 (1994).
[2] T. Nattermann and S. Scheidl, Adv. Phys. **49**, 607 (2000).
[3] D. R. Nelson and V. M. Vinokur, Phys. Rev. B **48**, 13060 (1993).
[4] T. P. Devereaux, R. T. Scalettar, and G. T. Zimanyi, Phys. Rev. B **50**, 13625 (1994).
[5] M. P. A. Fisher, Phys. Rev. Lett. **62**, 1415 (1989).
[6] D. S. Fisher, M. P. A. Fisher, and D. A. Huse, Phys. Rev. B **43**, 130 (1991).
[7] T. Giamarchi and P. Le Doussal, Phys. Rev. B **52**, 1242 (1995); see also T. Nattermann, Phys. Rev. Lett. **64**, 2454 (1990).
[8] C. A. Bolle, V. Aksyuk, F. Pardo, P. L. Gammel, E. Zeldov, E. Bucher, R. Boie, D. J. Bishop, and D. R. Nelson, Nature (London) **399**, 43 (1999).
[9] T. Giamarchi and H. J. Schulz, Europhys. Lett. **3**, 1287 (1987); Phys. Rev. B **37**, 325 (1988).
[10] T. Hwa, D. R. Nelson, and V. M. Vinokur, Phys. Rev. B **48**, 1167 (1993).
[11] J. L. Cardy and S. Ostlund, Phys. Rev. B **25**, 6899 (1982).
[12] J. Toner and D. P. DiVincenzo, Phys. Rev. B **41**, 632 (1990).
[13] T. Hwa and D. S. Fisher, Phys. Rev. Lett. **72**, 2466 (1994).
[14] C. L. Kane and M. P. A. Fisher, Phys. Rev. B **46**, 15233 (1992); see also S. Eggert and I. Affleck, *ibid.* **46**, 10866 (1992).
[15] I. Affleck, W. Hofstetter, D. R. Nelson, and U. Schollwöck, J. Stat. Mech.: Theory Exp. **2004**, 10003 (2004).
[16] D. R. Nelson, Phys. Rev. Lett. **60**, 1973 (1988); D. R. Nelson and H. S. Seung, Phys. Rev. B **39**, 9153 (1989).
[17] W. Hofstetter, I. Affleck, D. R. Nelson, and U. Schollwöck, Europhys. Lett. **66**, 178 (2004).
[18] A. Glatz and T. Nattermann, Phys. Rev. Lett. **88**, 256401 (2002).
[19] T. Bellini, L. Radzihovsky, J. Toner, and N. A. Clark, Science **294**, 5544 (2001).
[20] T. A. Vilgis, Phys. Rep. **336**, 167 (2000).
[21] See, e.g., D. S. Fisher, in *Phase Transitions and Relaxation in Systems with Competing Energy Scales*, edited by T. Riste and D. Sherrington (Kluwer Academic Publishers, Boston, 1993).
[22] S. F. Edwards and P. W. Anderson, J. Phys. F: Met. Phys. **5**, 965 (1975).
[23] J. Cardy, *Scaling and Renormalization in Statistical Physics* (Cambridge University Press, Cambridge, 1996).
[24] L. Lewin, *Polylogarithms and Associated Functions* (North-Holland, New York, 1981).
[25] P. Le Doussal and T. Giamarchi, Phys. Rev. Lett. **74**, 606 (1995).
[26] C. Zeng, A. A. Middleton, and Y. Shapir, Phys. Rev. Lett. **77**, 3204 (1996).
[27] S. Sachdev, *Quantum Phase Transitions* (Cambridge University Press, Cambridge, 1999).
[28] N. Hatano and D. R. Nelson, Phys. Rev. B **56**, 8651 (1997); see also M. Kardar and D. R. Nelson, Phys. Rev. Lett. **55**, 1157 (1985); M. Kardar, Nucl. Phys. B **290**, 582 (1992).
[29] H. J. Schulz, B. I. Halperin, and C. L. Henley, Phys. Rev. B **26**, 3797 (1982).
[30] Because in the disorder free case the eigenvalues of $\mathcal{T}$ come in degenerate pairs, weak disorder will not necessarily strongly lift this degeneracy. However, this issue is unimportant if we require that in finite system the filling factor is such that these degenerate or nearly degenerate pairs of states are either simultaneously filled or empty.